PCCP

PAPER

View Article Online
View Journal

Cite this: DOI: 10.1039/c4cp04530k

The chain conformation and relaxation dynamics of poly(acrylic acid)-*graft*-poly(ethylene oxide)-*graft*-dodecyl in water: effect of side-chains and distribution of counterions

Jingliang Li and Kongshuang Zhao*

We present a study on the dielectric behavior of an aqueous solution of an amphiphilic copolymer, poly(acrylic acid)-*graft*-poly(ethylene oxide)-*graft*-dodecyl (PAA-*g*-PEO-*g*-dodecyl), in the frequency range of 40 Hz to 110 MHz at varying concentrations and temperatures. After eliminating the electrode polarization at low-frequency, three dielectric relaxation processes were observed at about 1.2 MHz, 150 kHz and 30 kHz, whose mechanisms were proved to originate from the fluctuations of free counterions, the fluctuation of condensed counterions, and the rotation of intramolecular aggregates, respectively. The concentration dependence of the dielectric increment $\Delta\varepsilon$ and relaxation time τ for these three relaxations presents an abrupt change at 0.15 mg ml^{-1}, indicating that PAA-*g*-PEO-*g*-dodecyl molecules undergo a conformational transition from intramolecular aggregates to intermolecular aggregates. Moreover, both $\Delta\varepsilon$ and τ show a clear transition at about 317 K, suggesting a partial collapse of the aggregates. The correlation length and the contour length of the PAA-*g*-PEO-*g*-dodecyl chain were estimated according to Ito's theory of counterion fluctuation. It was found that the hydrophobic/hydrophilic side-chains affected the microscopic conformation of PAA, and the hydrogen-bond interactions greatly influenced the conformation. Additionally, the activation energy of these three relaxations was calculated and the process of ionic conduction was studied and the results were used to discuss counterion distribution and ion conduction.

Received 7th October 2014,
Accepted 10th December 2014

DOI: 10.1039/c4cp04530k

www.rsc.org/pccp

1. Introduction

Extensive attention has been paid to the self-association behaviors of graft copolymers containing hydrophobic/hydrophilic side-chains over the last two decades.[1–5] This kind of copolymer can form aggregates or polymeric micelles at very low concentration,[2–4] and their structure is sensitive to changes in the content of the side-chains, temperature and pH of the solution.[3–5] These properties of the copolymers give them potential wide-applicability in the field of drug delivery.[6]

Recently, Hao *et al.*[5] reported a kind of graft copolymer, poly(acrylic acid)-*graft*-poly(ethylene oxide)-*graft*-dodecyl (PAA-*g*-PEO-*g*-dodecyl), which contains both hydrophobic and hydrophilic side-chains. They found these copolymers can easily form aggregates in water spontaneously, owing to the hydrogen-bond interactions between the carboxyl groups on the PAA main-chain and PEO side-chains and the hydrophobic interactions among the dodecyl side-chains. Therefore, these copolymers have been studied as novel types of carriers in drug delivery systems. For example, the hydrophobic microdomains formed by the dodecyl side-chains can package hydrophobic drugs[4,5] and the carboxyl groups can load cationic drugs. In addition, the content of PEO/dodecyl, the solution pH and the preparation steps of the polyelectrolyte solution will control the micro-structure of the aggregates and dynamics of the solution.[5] As a result, this will significantly affect the function of PAA-*g*-PEO-*g*-dodecyl as a drug carrier.[6,7] Therefore, investigating the conformation of PAA-*g*-PEO-*g*-dodecyl and its dynamics in water can not only provide fundamental guidance for the design and preparation of these copolymers to put them into a special-purpose application, but also contribute to a better understanding of the self-assembly property of similar amphiphilic copolymers.

From a fundamental viewpoint, PAA-*g*-PEO-*g*-dodecyl is a polyelectrolyte of typical structure, where hydrophilic PEO and hydrophobic dodecyl side-chains were grafted onto the PAA main-chain. Its chain conformation is determined by the competition among the electrostatic, hydrogen-bond and hydrophobic interactions. Exploring how the various interactions affect the chain conformation will promote the understanding of the nature of the complexity of polyelectrolyte solutions. In the last two decades, a large number of studies on polyelectrolyte solutions have been

College of Chemistry, Beijing Normal University, Beijing 100875, China.
E-mail: zhaoks@bnu.edu.cn

reported, and most attention has been paid to the chain conformation,[8–10] distribution of counterions and their dynamics.[11–13] Among these studies, the concept of electrostatic blob was widely employed to describe the conformation of the polyelectrolyte chains,[9,14] and many parameters that describe the chain conformation, the scaling behaviors and the power-law relationship between the end-to-end distance (the contour length) and the concentration (or the degree of polymerization and the fraction of charged monomer) have been derived.[9,14,15] However, most of this research mainly focused on theoretical discussions of the structure and dynamics of polyelectrolyte solutions as described above, and the experimental studies which can support the theory are relatively backward. In particular, there are relatively few reports that discuss the effect of the hydrophobic/hydrophilic side-chains on the microscopic conformation of the polyelectrolyte chain from the scaling relations. Therefore, whether or not the existing scaling theory can explain the conformation of the polyelectrolyte chain containing hydrophobic/hydrophilic side-chains and how the intra- and inter-molecular interactions introduced by side-chains affect the chain conformation, are both questions that are worthwhile to explore.

On the other hand, the spatial distribution of counterions, namely, how the counterions distribute in the vicinity of the polyelectrolyte chain and in the bulk solution, has always been the focus of the fundamental research on polyelectrolyte solutions. That is because the counterions regulate various intramolecular and intermolecular interactions and consequently determine the conformation of the polyelectrolyte chain.[10,15] The distributions of counterions in dilute and semi-dilute solutions have been well described by two models: the two-state model proposed early by Oosawa–Manning[16] and the two-zone model proposed recently by Deshkovski–Obukhov–Rubinstein.[9,17] In these theoretical models, the counterions are divided into two kinds, one called condensed counterions which are tightly bound in the vicinity of the fixed charge on the chain (see the shadow in Fig. 1); the other called free counterions that are far away from the main-chain, including the loosely bound counterions distributed within a wide range between the chains (within dashed circle) and those totally free counterions in bulk water. These counterions show different abilities in movement and conductivity under an electric field,[16,18] since the counterions are subjected to different electrostatic interactions from the fixed charges on the main-chain. Exploring the contributions of these counterions to the dynamics of polyelectrolyte solutions in different time scales is also an important issue.

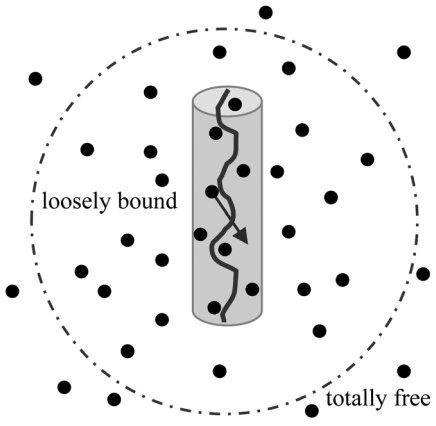

Fig. 1 Distribution of counterions in polyelectrolyte solutions, including the tightly bound condensed counterions in the vicinity of fixed charge on the main-chain, the loosely bound free counterions, and those totally free counterions in bulk water.

Dielectric relaxation spectroscopy (DRS), owing to its sensibility to all kinds of polarization processes, has been used to detect the fluctuation of dipoles, the movements of molecules or ions[19–21] and to provide valuable information on charge distribution, intermolecular interactions and conformational changes.[21,22] In fact, theoretical studies about the dielectric property of polyelectrolyte solutions had begun very early as reviewed by Mandel.[23] Two relaxation processes occurring in the range of MHz and kHz, which can be explained using the existing theories, are usually observed over the radio frequency range.[20] Although there have been some controversies over the identity of these two relaxations for a long time, currently the general consensus is that they are attributed to the fluctuation of free counterions and condensed counterions. This identification is based on the counterion fluctuation theory which was firstly proposed by Ito[19] and developed by Cametti.[24,25] According to this theory, the dielectric behavior of some polyelectrolyte solutions has been explained well,[26–28] as in our recent study in which the dielectric relaxations of PAA, PAA-*g*-dodecyl and PAA-*g*-PEO solutions were well described by the theory of counterion fluctuation. It was suggested that the dielectric behaviors of polyelectrolyte solutions at radio frequency range are mainly determined by the fluctuation of counterions along or away from the chains. It was also found that one more relaxation occurring in the range of kHz occurs in the PAA-*g*-PEO solutions than in PAA (or PAA-*g*-dodecyl) solutions, and this extra relaxation is related to the aggregates formed in PAA-*g*-PEO solutions. As for PAA-*g*-PEO-*g*-dodecyl, a kind of graft copolymer with novel structure, it is expected that the relaxation processes that will occur in the radio frequency range and the reason for the relaxations will be discovered.

To this end, we carried out dielectric measurements on the PAA-*g*-PEO-*g*-dodecyl aqueous solution over a frequency range from 40 Hz to 110 MHz. We focused on the dielectric relaxation mechanisms and the aggregate structure of PAA-*g*-PEO-*g*-dodecyl when the systems are exposed to changes in the concentration and temperature. Notably, we demonstrated the effect of hydrophobic/hydrophilic side-chains on the microscopic conformation of the PAA main-chain, based on the scaling theory of polyelectrolytes. We also calculated the activation energy of ionic conductivity from analyzing the temperature-dependence of the dielectric spectra. Based on the dielectric analysis, the counterion distribution around the PAA-*g*-PEO-*g*-dodecyl main chain was discussed from the thermodynamical viewpoint, and their contributions to the relaxation processes owing to the different degree of constrain by fixed charges were confirmed.

2. Experimental section

2.1. Materials

Solid samples of PAA-*g*-PEO-*g*-dodecyl were supplied by Hao Jinkun from the Chinese Academy of Sciences (Beijing, P. R. China). The PEO (M_w: 2000 g mol^{-1}) and dodecyl side chains were grafted onto the PAA (M_w: 250 000 g mol^{-1}) main-chain according to the classical reaction of amino with carboxylic groups. The structure of the copolymer is shown in Scheme 1. The procedure of preparing the sample and the characterization of its composition has been reported in the recent work of Hao.[5] The weight percents of PEO and dodecyl are 12% and 7%, respectively, which equates to 0.27% and 5.9% in the molar fraction of the monomer.

PAA-*g*-PEO-*g*-dodecyl solid samples were firstly dissolved in 2.0 ml DMF, and then diluted by doubly distilled water (specific resistance higher than 16 MΩ cm^{-1}) to 50 ml with the help of a glass rod. Solutions of different concentration from 1.0 to 0.03 mg ml^{-1} were obtained. The pH of all these solutions was adjusted to about 7.0 using a 0.5 mol L^{-1} NaOH solution.

2.2. Dielectric measurements

The complex dielectric permittivity ε^* ($= \varepsilon - j\varepsilon''$, where ε and ε'' are permittivity and dielectric loss, respectively) of the PAA-*g*-PEO-*g*-dodecyl solutions was measured using a 4294A Precision Impedance Analyzer (Agilent Technologies) from 40 Hz to 110 MHz, controlled by a personal computer. The applied alternating field was 500 mV and a dielectric measuring cell with concentrically cylindrical platinum electrodes (the effective area of the electrodes was 78.5 mm^2 and the electrode distance was 8 mm) was employed to load the samples. The concentration dependence dielectric measurements were carried out at 21.2 ± 0.2 °C (the room temperature) and the temperature dependence measurements were performed from 7.7 to 73.5 °C, controlled by a circulating thermostatic water jacket. The raw experimental data, capacitance C_x and conductance G_x, were corrected by the cell constant C_r, stray capacitance C_l and residual inductance L_r (arising from the terminal leads) based on the following equations according to Schwan's method:[29]

$$C_s = \frac{C_x\left(1+\omega^2 L_r C_x\right)+L_r {G_x}^2}{\left(1+\omega^2 L_r C_x\right)^2+\left(\omega L_r G_x\right)^2} - C_r \quad (1a)$$

$$G_s = \frac{G_x}{\left(1+\omega^2 L_r C_x\right)^2+\left(\omega L_r G_x\right)^2} \quad (1b)$$

where C_s and G_s denote the modified values, respectively. ω ($= 2\pi f$, f is the measurement frequency) is the angular frequency. The values of C_l (= 0.480 pF) and C_r (= 0.109 pF) were determined with pure water, ethanol and air. The value of L_r was determined by use of standard KCl solutions with different concentrations.[29] Then the permittivity ε and conductivity κ were determined using the equations $\varepsilon = C_s/C_l$ and $\kappa = G_s\varepsilon_0/C_l$ (where $\varepsilon_0 = 8.8541 \times 10^{-12}$ F m^{-1}, is the vacuum permittivity).

2.3. Dielectric analysis

In an applied electric field of frequency f, the dielectric property of an aqueous polyelectrolyte solution can generally be characterized in terms of the complex permittivity ε^*:

$$\varepsilon^* = \varepsilon - \frac{j\kappa}{\omega\varepsilon_0} = \varepsilon - j\left(\varepsilon'' + \frac{\kappa_l}{\omega\varepsilon_0}\right) \quad (2)$$

Here ε denotes the relative permittivity, which is called permittivity for short hereinafter, κ the conductivity, κ_l the low-frequency limits of conductivity (or called the dc conductivity), ω($= 2\pi f$) the angular frequency, and $j = (-1)^{1/2}$. In the polyelectrolyte solution, usually the total dielectric loss contains the effective dielectric loss of the sample and the dc conductivity contribution. The contribution of dc conductivity κ_l can be subtracted from the conductivity spectra using the following equation:

$$\varepsilon'' = \frac{(\kappa - \kappa_l)}{\omega\varepsilon_0} \quad (3)$$

In this work κ_l was read out from the platform of the conductivity spectra at several kHz.

The whole dielectric spectrum free of the dc conductivity effect was analyzed using following empirical equation including the Cole–Cole's terms and the electrode polarization (EP) term:[29,30]

$$\varepsilon^* = \varepsilon_h + \sum_i \frac{\Delta\varepsilon_i}{1+(j\omega\tau_i)^{\alpha_i}} + A\omega^{-m} \quad (4)$$

where $\Delta\varepsilon_i$ is the dielectric increment (or relaxation intensity) of the relaxation i. The difference in the platform values between the adjacent two relaxations, *i.e.* $\Delta\varepsilon_i(= \varepsilon_{il} - \varepsilon_{ih})$, ε_{il} and ε_{ih}, are the low- and high-frequency limits of the permittivity of the relaxation i, respectively. $\tau = 1/2\pi f_0$ is the characteristic relaxation time (f_0 is the characteristic relaxation frequency) and $\alpha(0 < \alpha \leq 1)$ is the shape parameter related to the distribution of relaxation times. $A\omega^{-m}$ (A and m are adjustable parameters) in eqn (4) takes into account the effect of electrode polarization (EP) on the permittivity, on the basis of the power-law frequency dependence method.[29,30] It was demonstrated in our recent work[28] that the EP mainly affects the real part of the permittivity, but has little effect on the imaginary part.

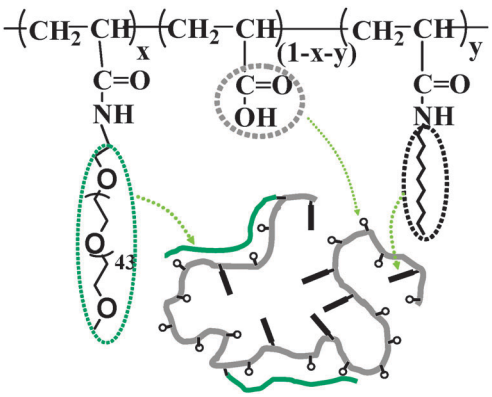

Scheme 1 Schematic illustrations of the structure of PAA-*g*-PEO-*g*-dodecyl molecules. PEO and dodecyl side-chains were randomly distributed on the PAA main-chain, whose molar fractions are 0.27% (*x*) and 5.9% (*y*), respectively.

In the process of dielectric analysis, firstly the corrected dielectric loss free of the effect of dc conductivity was obtained using eqn (3). Then, it is an important procedure to eliminate the contribution of EP that may obscure possible relaxations at low-frequency. To this end, we fitted eqn (4) to the raw permittivity data and corrected the dielectric loss (using eqn (3)) simultaneously, and parameters A and m of the EP term were determined. Thus, a new ε-curve without the EP effect was derived by mathematically subtracting the $A\omega^{-m}$ from the raw permittivity. Finally, the dielectric parameters $(\Delta\varepsilon,\tau,\alpha)$ were determined by simultaneously fitting the Cole–Cole equation with the corrected permittivity and the corrected dielectric loss.[26] The optimized fitting curves were guaranteed by the nonlinear least-squares method.

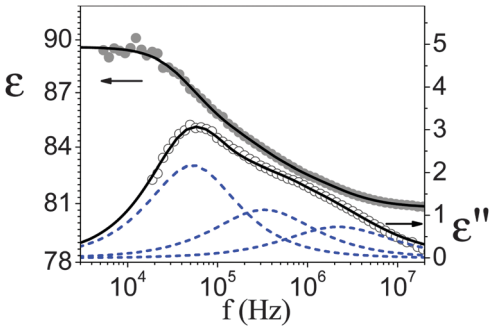

Fig. 3 A typical fitting result of the spectrum of PAA-*g*-PEO-*g*-dodecyl solution at 0.6 mg ml^{-1}. The corrected permittivity (solid circles) and the dielectric loss (open circles) were obtained by subtracting the EP effect from the original spectrum according to the method described in Section 2.3.

3. Results and discussion

3.1. Dielectric spectra of PAA-*g*-PEO-*g*-dodecyl solutions of different concentrations

Fig. 2 shows the permittivity after eliminating the EP effect by the method introduced in Section 2.3. From Fig. 2 a widely distributed relaxation can be observed in the frequency range from 10 kHz to 100 MHz, suggesting there are two or more sub-relaxation processes. It is interesting to find that within the experimental concentration range (0.03–1.0 mg ml^{-1}), the spectra were divided into two groups: 0.03–0.1 mg ml^{-1} and 0.2–1.0 mg ml^{-1}, and the dielectric data in these two groups were obviously at different levels.

The dielectric spectra of the PAA-*g*-PEO-*g*-dodecyl solutions of all concentrations were all well represented by the Cole–Cole equation containing three relaxation terms with the best-fit relaxation parameters. Fig. 3 shows a representative fitting result of the PAA-*g*-PEO-*g*-dodecyl solution at a concentration of 0.6 mg ml^{-1} and the obtained relaxation parameters are summarized in Table 1. It is clearly seen that the dielectric spectrum contains three sub-relaxation processes, whose relaxation times were: 160 ns (about 1.2 MHz, called high-frequency (HF) relaxation), 1 μs (about 150 kHz, called middle-frequency (MF) relaxation) and 5 μs (about 30 kHz, called low-frequency (LF) relaxation). The three distribution parameters of relaxation time, α_l, α_m and α_h, are close to 1, around 0.9 and 0.80, respectively, indicating that the low-frequency relaxation is the Debye-type relaxation indicating the unity of the relaxation mechanism, while the middle- and high-frequency relaxations show some distribution which may originate from the heterogeneity in the microscopic conformation of the polyelectrolyte chain.[31] Specifically, the electrostatic blob (see Fig. 6 below) near the center of the chain experiences stronger electrostatic repulsion than the blob closer to the chain ends, thus the size of the electrostatic blobs is not uniform (the smallest blob is in the middle of the chain). As a result, the correlation length ξ and the chain contour length L (see Fig. 6) may be different for each polyelectrolyte chain, which leads to the non-uniformity in relaxation time, *i.e.* the relaxation time exhibits some distributions.

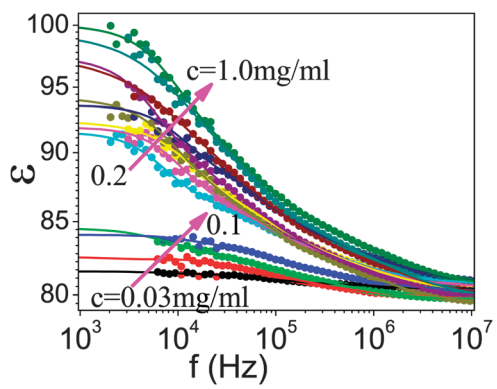

Fig. 2 The permittivity of PAA-*g*-PEO-*g*-dodecyl solutions after eliminating the EP effect.

3.2. Conformation of the PAA-*g*-PEO-*g*-dodecyl molecule at different concentrations

Fig. 4 shows the concentration dependence of the dielectric parameters of these three sub-relaxations in PAA-*g*-PEO-*g*-dodecyl solutions. It can be seen from the data of the dielectric increment and the relaxation time that there is a transition at the concentration of 0.15 mg ml^{-1}, which is consistent with the concentration in Fig. 2 that divides the dielectric spectra into two groups. This result indicates a sudden transition of the conformation of the PAA-*g*-PEO-dodecyl molecule or the type of aggregate at 0.15 mg ml^{-1}. This speculation was confirmed by the light scattering experiment of Hao,[5] which showed that at low concentrations, PAA-*g*-PEO-*g*-dodecyl exists in the form of intramolecular aggregates, owing to the intramolecular hydrogen bonding between PAA and PEO and the hydrophobic interactions among dodecyl side-chains.[5] While at slightly higher concentrations, the PAA-*g*-PEO-*g*-dodecyl molecules are entangled with each other and the intermolecular interactions dominate and as a result, the intermolecular aggregates dominate in PAA-*g*-PEO-*g*-dodecyl solutions. According to Hao *et al.*,[32] the critical aggregation concentration of a PAA-*g*-PEO-*g*-dodecyl solution is estimated to be about 0.2 mg ml^{-1} when the weight of dodecyl and PEO are 12% and 7%, respectively (the same as the sample used in this work), and this concentration is close to the transition concentration (0.15 mg ml^{-1})

Table 1 Dielectric parameters of the relaxations in PAA-*g*-PEO-*g*-dodecyl solutions of different concentrations, obtained by fitting eqn (4) with the dielectric spectra

c (mg ml^{-1})	$\Delta\varepsilon_l$	$\Delta\varepsilon_m$	$\Delta\varepsilon_h$	τ_l ($\mp$s)	τ_m ($\mp$s)	τ_h (ns)	α_l	α_m	α_h
0.03	0.51 ± 0.03	0.427 ± 0.03	0.291 ± 0.01	7.11 ± 0.5	1.53 ± 0.1	178 ± 5	0.99 ± 0.1	0.98 ± 0.2	0.71 ± 0.2
0.05	0.616 ± 0.03	0.792 ± 0.03	1.27 ± 0.05	4.86 ± 0.3	1.4 ± 0.1	346 ± 8	0.99 ± 0.1	0.89 ± 0.3	0.72 ± 0.2
0.08	0.846 ± 0.04	1.18 ± 0.05	1.32 ± 0.05	3.71 ± 0.3	1.01 ± 0.1	227 ± 6	0.98 ± 0.2	0.85 ± 0.3	0.72 ± 0.
0.1	0.963 ± 0.04	1.21 ± 0.05	1.65 ± 0.05	6.75 ± 0.5	1.43 ± 0.1	245 ± 6	0.98 ± 0.2	0.94 ± 0.5	0.75 ± 0.3
0.2	1.79 ± 0.1	2.57 ± 0.1	2.44 ± 0.1	6.65 ± 0.5	1.52 ± 0.1	215 ± 5	0.99 ± 0.1	0.87 ± 0.3	0.75 ± 0.2
0.3	3.33 ± 0.1	2.67 ± 0.1	1.97 ± 0.1	5.91 ± 0.4	1.08 ± 0.1	140 ± 4	0.98 ± 0.2	0.89 ± 0.3	0.83 ± 0.3
0.4	3.92 ± 0.1	2.23 ± 0.1	2.73 ± 0.1	5.14 ± 0.4	1.02 ± 0.1	142 ± 4	0.99 ± 0.1	0.98 ± 0.5	0.82 ± 0.3
0.5	4.53 ± 0.1	3.01 ± 0.1	2.7 ± 0.1	6.13 ± 0.4	1.08 ± 0.1	120 ± 3	0.98 ± 0.2	0.92 ± 0.4	0.84 ± 0.3
0.6	4.13 ± 0.1	3.13 ± 0.1	2.45 ± 0.1	4.45 ± 0.3	0.836 ± 0.07	98.9 ± 3	0.98 ± 0.2	0.89 ± 0.3	0.81 ± 0.23
0.7	4.41 ± 0.1	2.48 ± 0.1	2.95 ± 0.1	4.81 ± 0.3	0.983 ± 0.07	121 ± 4	0.99 ± 0.1	0.95 ± 0.4	0.83 ± 0.2
0.8	5.75 ± 0.2	3.72 ± 0.1	3.15 ± 0.1	6.22 ± 0.4	1.04 ± 0.1	98.2 ± 3	0.98 ± 0.2	0.92 ± 0.4	0.83 ± 0.
0.9	6.38 ± 0.2	3.3 ± 0.1	3.34 ± 0.1	4.88 ± 0.3	0.839 ± 0.08	87.4 ± 2	0.98 ± 0.2	0.94 ± 0.5	0.84 ± 0.4
1	5.87 ± 0.2	4.45 ± 0.1	3.71 ± 0.1	5.21 ± 0.4	1.14 ± 0.1	86 ± 2	0.98 ± 0.2	0.87 ± 0.3	0.80 ± 0.2

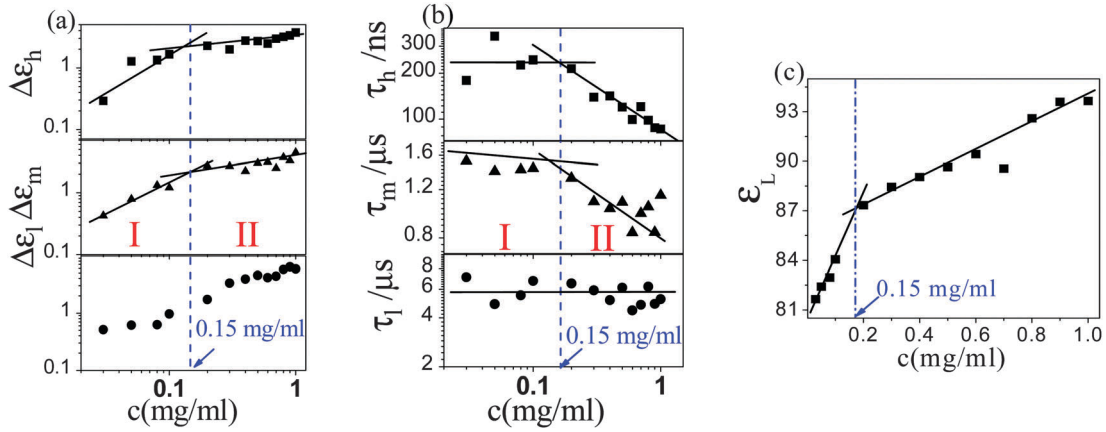

Fig. 4 Concentration dependence of dielectric increment $\Delta\varepsilon_i$ (a), relaxation time τ_i (b) and static permittivity ε_L (c) of PAA-*g*-PEO-*g*-dodecyl solution. Here, ε_L denotes the static permittivity, which is equal to the permittivity at low-frequency.

reported in our work. Consequently, we can conclude that at the concentration range of 0.03–0.1 mg ml^{-1} (called region I), the intramolecular aggregation of the hydrophobic side chains results in a micelle-like structure, as shown in the left side of Fig. 5; while at the concentration range of 0.2–1.0 mg ml^{-1} (called region II), the entanglement of the chains leads to the formation of intermolecular aggregates as illustrated in the right side of Fig. 5. The concentration of 0.15 mg ml^{-1} is often known as the overlap concentration (c^*) because from this concentration the PAA-*g*-PEO-*g*-dodecyl molecules start to entangle with each other.[14] It should be noted here that this overlap concentration is much smaller than that of a PAA (M_w = 250 000 g mol^{-1}) solution at pH ≈ 7.0, which is about 1 mg ml^{-1}, obtained from the viscosity and dynamic light scattering (DLS) measurements in Litmanovich's work.[33] This result is quite predictable because hydrophilic/hydrophobic side chains greatly strengthen the interactions among PAA-*g*-PEO-*g*-dodecyl molecules, thus PAA-*g*-PEO molecules start to overlap at a very low concentration.

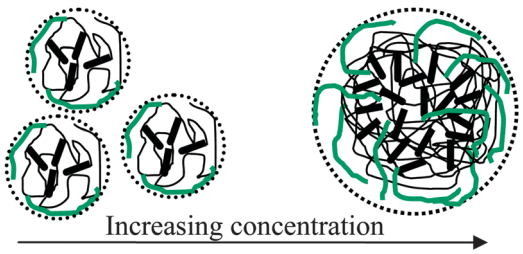

Fig. 5 Schematic of possible conformations of PAA-*g*-PEO-*g*-dodecyl molecules with increasing concentration.

3.3. Effect of side chains on the conformation of PAA-*g*-PEO-*g*-dodecyl

There is an accepted judgment about the relaxation mechanism of polyelectrolyte solutions, that the fluctuation of counterions will cause relaxations at radio-frequency range.[19,20] The relaxation strength, especially the relaxation frequency, depends on the fluctuation distance of the counterions[19] and this distance is determined by the micro conformation of the polyelectrolyte chain. In order to identify the mechanism of these three relaxations in this work, and then explore the micro conformation of PAA-*g*-PEO-*g*-dodecyl molecules in water, we employed the electrostatic blob model of Rubinstein.[9,14]

Fig. 6 shows the electrostatic blob model of a polyelectrolyte chain in dilute and semi-dilute solutions. In the model, each electrostatic blob is of size D and contains several monomers.

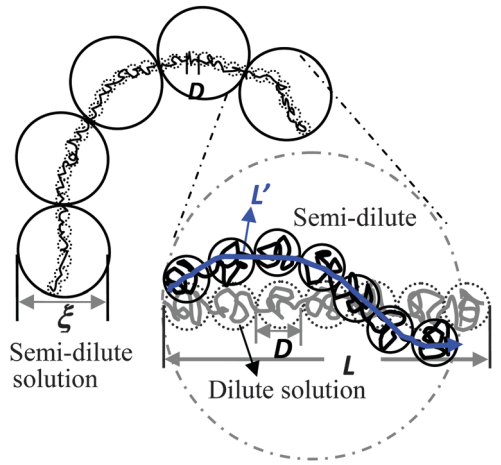

Fig. 6 Electrostatic blob model of a polyelectrolyte chain. D is the size of the blobs, L is the chain contour length in dilute solutions and ξ is the correlation length in semi-dilute solutions. Here we define L' as the chain contour length in semi-dilute solutions, whose value is close to L in dilute solutions.

In dilute solutions, the polyelectrolyte chain adopted an entirely extended configuration of electrostatic blobs with length L (see the dotted circle in Fig. 6). Here L denotes the chain contour length in dilute solutions. In semi-dilute solutions, their major feature is the existence of the correlation length ξ. On length scales smaller than ξ, the chain adopted an extended configuration which is similar to that in dilute solutions; while on longer length scales (>ξ), the chain is a random walk defined by the correlation length ξ (see the solid circle in Fig. 6).[14] In this work we define L' as the contour length of the polyelectrolyte chain in semi-dilute solutions (see blue arrow in Fig. 6). The value of L' is close to L because they both approximate to the total length of the electrostatic blobs.

As the concentration of polyelectrolyte increases, the enhanced electrostatic shielding, owing to the increasing concentration of ions, screens the electrostatic repulsion between the electrostatic blobs. Therefore, the extension of the electrostatic blobs is weakened and the correlation length ξ decreases. According to the scaling theory of polyelectrolyte solutions,[8,14,24] the ξ shows the following scaling relationship with the polyelectrolyte concentration c:[8,14,19,24]

$$\xi \approx L(c/c^*)^{-1/2} \quad (5)$$

where c^* is the overlap concentration. When $c = c^*$, the correlation length ξ in semi-dilute solutions is equal to the contour length L in dilute solutions.

As for the relaxation in the range of MHz (the HF relaxation in this work), Ito and Bordi *et al.*[19,20,23] attributed it to the fluctuation of free counterions (the loosely bound counterions defined in Fig. 1) within the correlation length ξ. Ito's theory of counterion fluctuation has been supported by many experiments.[25–27] According to Ito, the relaxation time of the fluctuation of free counterions τ_{ion} can be expressed by the following equation:[24,25]

$$\tau_{ion} = \frac{\xi^2}{6D_{ion}} \quad (6)$$

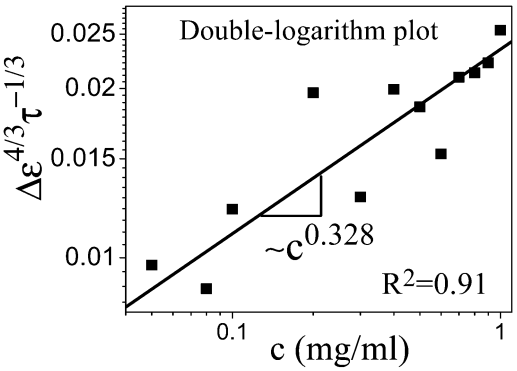

Fig. 7 Plot of $\log \Delta\varepsilon_h{}^{4/3}\tau_h{}^{-1/3}$ against $\log c$, according to the dielectric parameters for the HF relaxation in Table 1.

where D_{ion} is the diffusion coefficient of counterions and ξ is the fluctuation distance of free counterions which corresponds to the correlation length in semi-dilute solutions.[14,19,20] Based on Ito's theory, Bordi *et al.*[24,34] have derived the scaling relation between the dielectric parameters and the polyelectrolyte concentration in different solvents. In this work, water is a poor solvent for the backbone of the PAA-*g*-PEO-*g*-dodecyl chain. According to Bordi *et al.*,[24,34] the dielectric increment ($\Delta\varepsilon_{ion}$) and relaxation time (τ_{ion}) that originates from the fluctuation of free counterions gives the following scaling relation with the concentration (c):

$$\Delta\varepsilon_{ion}{}^{4/3}\tau_{ion}{}^{-1/3} \propto c^{1/3} \quad (7)$$

Fig. 7 shows the plot of $\log \Delta\varepsilon_h{}^{4/3}\tau_h{}^{-1/3}$ against $\log c$ according to eqn (7) based on the dielectric parameters of the HF relaxation in Table 1. From Fig. 7 a good linear relationship between $\log \Delta\varepsilon_h{}^{4/3}\tau_h{}^{-1/3}$ and $\log c$ can been seen, and its slope is 0.328 which is very approximate to the theoretical value, 1/3, predicted from eqn (7). This result suggests that the HF relaxation (around 1.2 MHz) for PAA-*g*-PEO-*g*-dodecyl solution originates from the fluctuation of free counterions. This is consistent with the conclusion obtained for similar polyelectrolyte solutions, PAA, PAA-*g*-PEO and PAA-*g*-dodecyl.[28,36]

According to eqn (6), the fluctuation distance (equivalent to the correlation length ξ) of counterions at different concentrations was calculated by substituting in the diffusion coefficient of Na^+ in water (1.33×10^{-9} m^2 s^{-1} (ref. 35)) and the HF relaxation time (from Table 1). Fig. 8 shows the double logarithmic plots of the correlation length ξ against the concentration c for PAA-*g*-PEO-*g*-dodecyl. Meanwhile, values of ξ for similar systems, PAA, PAA-*g*-PEO and PAA-*g*-dodecyl were also calculated and the results are also presented in Fig. 8. It can be seen from Fig. 8 that for PAA, the correlation length ξ shows the scaling relationship $\xi \propto c^{-0.487}$, being well consistent with the theoretical prediction of chain conformation $\xi \propto c^{-0.5}$ (from eqn (5)).[14,34] However, for the polyelectrolyte containing side-chains, the scaling exponents between ξ and c are −0.390 (for PAA-*g*-dodecyl), −0.286 (for PAA-*g*-PEO) and −0.256 (for PAA-*g*-PEO-*g*-dodecyl), respectively, which deviate from the theoretical value (−0.5) predicted from eqn (5). This means that grafting hydrophilic/hydrophobic side-chains onto

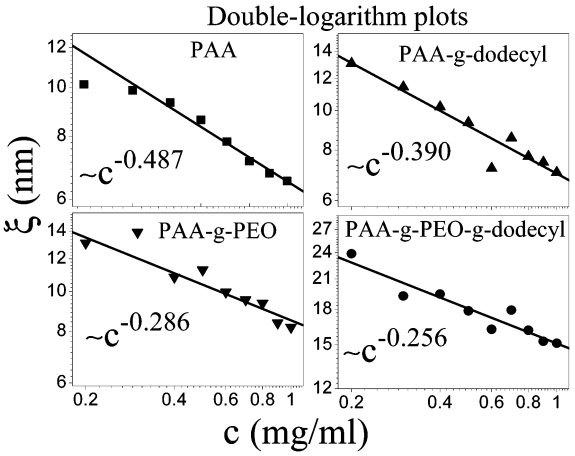

Fig. 8 Concentration dependence of the correlation length ξ in PAA, PAA-*g*-PEO, PAA-*g*-dodecyl and PAA-*g*-PEO-*g*-dodecyl solutions.

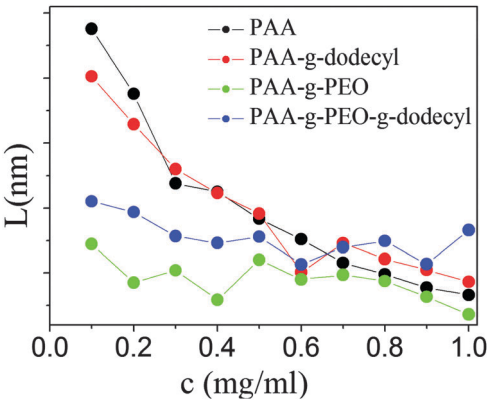

Fig. 9 Concentration dependence of the chain contour length *L* for PAA, PAA-*g*-PEO, PAA-*g*-dodecyl and PAA-*g*-PEO-*g*-dodecyl.

the PAA main-chain significantly affects the microscopic conformation of the PAA chain in water. It is interesting to note that grafting hydrophilic PEO causes a larger deviation from the theoretical value than grafting hydrophobic dodecyl, which indicates that the hydrogen bonding between PAA and PEO has a greater impact on the microscopic conformation of PAA. Moreover, for the polyelectrolyte with side chains, the decreasing rates of the correlation length with the concentration are smaller than the theoretical prediction of eqn (5). This may be because the introduction of PEO or dodecyl side-chains strengthens the interactions among the PAA chains, which weakens the effect of the increasing electrostatic shielding to a certain degree, and as a result, the decreasing of the correlation length with increasing concentration is blocked.

With respect to the middle-frequency relaxation around 150 kHz for PAA-*g*-PEO-*g*-dodecyl solutions, it can be verified as a direct consequence of the fluctuation of condensed counterions (the tightly bound counterions defined in Fig. 1), based on the results of our previous work.[28,36] According to Brodi *et al.*,[20,27] the relaxation time τ_{cond} for fluctuation of condensed counterions is given by the following equation:[20]

$$\tau_{cond} \approx \frac{\zeta_f L^2}{6k_B T} \quad (8)$$

where, k_BT is the thermal energy, ζ_f is the friction coefficient of condensed counterions moving along the polyelectrolyte backbone, and L is the fluctuation distance of condensed counterions which is equal to the chain contour length.[20] Taking the contour length L to be 100 nm from the literature[28,37] and substituting the friction coefficient of Na^+ ($\zeta_{Na^+} = 5.2 \times 10^{-12}$ kg s^{-1})[38] into eqn (8), the relaxation time τ_{cond} for the fluctuation of condensed counterion was calculated to be 0.21 μs (equivalent to 75 kHz in frequency), which is not a value remarkably different compared with the experimental value 150 kHz in this work. This confirms the above speculation that the middle-frequency relaxation for PAA-*g*-PEO-*g*-dodecyl solution is caused by the fluctuation of condensed counterions.

By substituting the relaxation time τ_{cond} for PAA, PAA-*g*-dodecyl, PAA-*g*-PEO, and PAA-*g*-PEO-*g*-dodecyl solutions into eqn (8), the contour length of these polyelectrolyte chains in different concentrations were estimated and the results are shown in Fig. 9. It is interesting to find that PEO and dodecyl side-chains have a different effect on the chain contour length: for PAA and PAA-*g*-dodecyl, L decreases with the increase in concentration, while for PAA-*g*-PEO and PAA-*g*-PEO-*g*-dodecyl which contain hydrophilic PEO side-chains, L changes little. These results indicate that the hydrogen-bonding introduced by the PEO side-chains significantly affects the microscopic conformation of PAA, while the effects of the hydrophobic interactions are relatively weak.

Additionally, as mentioned above, usually just two relaxation processes can be observed for polyelectrolyte solutions,[20] but in this work one more relaxation at about 30 kHz was observed for PAA-*g*-PEO-*g*-dodecyl solutions. We deduce that this extra relaxation probably relates to the aggregates in PAA-*g*-PEO-*g*-dodecyl solutions owing to the existence of PEO/dodecyl side-chains. Considering PAA-*g*-PEO-*g*-dodecyl molecules are in the form of aggregates in water,[5] the aggregates can be approximately modeled as spherical particles, thus, the rotational relaxation time τ_{rot} can be estimated by the Stokes–Einstein–Debye (SED) theory:[39,40]

$$\tau_{rot} = \frac{4\pi\eta R_h^3}{k_B T} \quad (9)$$

where, the hydrodynamic radius R_h is about 14 nm, obtained from the light scattering experiment of Hao *et al.*,[5] η is the solvent viscosity which is equal to 0.97×10^{-3} Ns m^{-2} at the experimental temperature 21.2 °C. Substituting them into eqn (9), the rotational relaxation time τ_{rot} was calculated to be 8.2 μs, being very close to 5 μs of the LF relaxation. This result suggests that the rotation of the intramolecular aggregates contributes to the low-frequency relaxation of PAA-*g*-PEO-*g*-dodecyl solutions. It should be noted here that the low-frequency relaxation may also originate from some other motions concerning the whole molecule.

3.4. Effects of temperature on the conformation of aggregates

In this work, temperature dependence dielectric measurements from 7.8 to 73.5 °C for a PAA-*g*-PEO-*g*-dodecyl solution were also

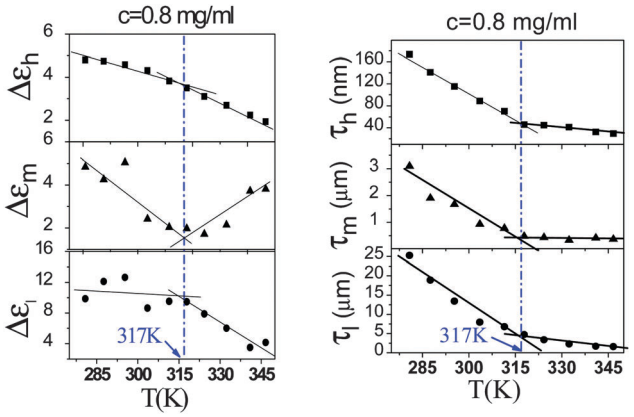

Fig. 10 Temperature dependence of the dielectric increment and the relaxation time of each sub-relaxation in the PAA-*g*-PEO-*g*-dodecyl solution at a concentration of 0.8 mg ml^{-1}.

carried out at a concentration of 0.8 mg ml^{-1} which is considered to be a semi-dilute solution. Within the experimental temperature range, the dielectric spectra at all temperatures were also well described by the Cole–Cole equation containing three relaxation processes and the dielectric parameters of these three sub-relaxations (called high-, middle- and low-frequency relaxation, respectively, as defined in Section 3.1) were obtained.

Fig. 10 shows the plots of dielectric increment and relaxation time of each sub-relaxation against the measuring temperature. It can be clearly seen that for each sub-relaxation, both the dielectric increment and the relaxation time present a transition at 317 K (44 °C), and this temperature is consistent with the transition in Fig. 11 that shows the temperature dependence of the low-frequency conductivity (κ_L) of PAA-*g*-PEO-*g*-dodecyl solutions. The interesting result in Fig. 11 suggests that the concentration of conducting ions suddenly increases when the temperature is above 317 K, or that the conformation of PAA-*g*-PEO-*g*-dodecyl changes at the specific temperature.

According to Hao *et al.*,[5] PAA-*g*-PEO-*g*-dodecyl molecules mainly exist in the form of intermolecular aggregates at the

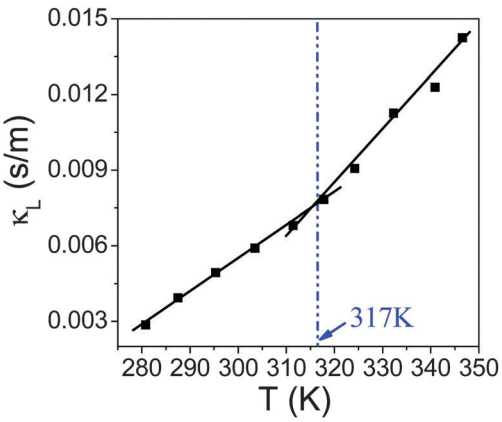

Fig. 11 Temperature dependence of the low-frequency conductivity of the PAA-*g*-PEO-*g*-dodecyl solution at the concentration of 0.8 mg ml^{-1}.

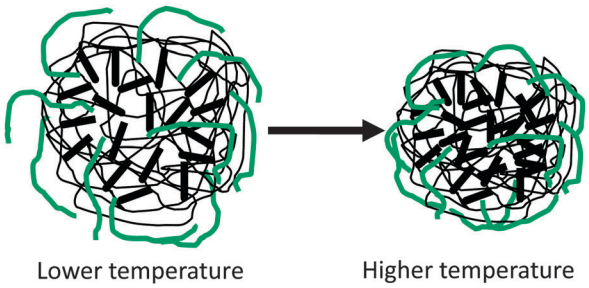

Fig. 12 The schematic illustration of the partial collapse of the aggregates in PAA-*g*-PEO-*g*-dodecyl solutions.

concentration of 0.8 mg ml^{-1}; therefore, the above results suggest a large change in the conformation of the intermolecular aggregates at the temperature of 317 K. Fig. 11 shows that the low-frequency conductivity (κ_L) of PAA-*g*-PEO-*g*-dodecyl solutions increases with the increasing temperature. More interestingly, the increasing rate of κ_L was accelerated when the temperature was above 317 K. This means the concentration of ions in PAA-*g*-PEO-*g*-dodecyl solution increases at certain temperatures, such as 317 K. We can infer that the aggregates partly collapse at temperatures above 317 K as illustrated in the following Fig. 12. As a result, some of the water molecules within the aggregates, together with some hydrated ions, are continually expelled from the aggregates as the temperature rises above 317 K, therefore, the number of ions that participate in the long-range migration increases, which leads to the sudden increase in the conductivity.

4. Conclusions

Dielectric behaviors of PAA-*g*-PEO-*g*-dodecyl solutions were investigated at different concentrations and temperatures, from 40 Hz to 110 MHz. After removing the effect of electrode polarization successfully, three sub-relaxation processes were confirmed and their dielectric parameters were determined. The mechanisms of the three sub-relaxations for PAA-*g*-PEO-*g*-dodecyl solutions, at about 1.2 MHz, 150 kHz and 30 kHz, were identified successfully, and were determined to have originated from the fluctuation of free counterions, the fluctuation of condensed counterions, and the rotation of intramolecular aggregates, respectively. It can be concluded that the dielectric behaviors of polyelectrolyte solutions at radio frequency are mainly dominated by the effects of counterions.

The special structure of PAA-*g*-PEO-*g*-dodecyl was demonstrated in this work. The transition in the relaxation time and dielectric increment at 0.15 mg ml^{-1} indicates that PAA-*g*-PEO-*g*-dodecyl molecules undergo a change from intramolecular aggregates to intermolecular aggregates, when the intermolecular hydrogen-bonds and hydrophobic interactions gradually become stronger than the intramolecular interactions. The temperature-dependent dielectric parameters show a transition at 317 K, suggesting that the aggregates partly collapse at temperatures above 317 K.

In addition, the conformational parameters, correlation length ξ and contour length L of the PAA-*g*-PEO-*g*-dodecyl chain were estimated according to Ito's counterion fluctuation theory. By systematically comparing the scaling behavior of PAA, PAA-*g*-PEO, PAA-*g*-dodecyl and PAA-*g*-PEO-*g*-dodecyl, we found that the effect of hydrogen-bonding, introduced by the PEO side-chains, on the conformation of the PAA main-chain is much greater than that of hydrophobic interactions. This work also provides an experimental support for the scaling theory of polyelectrolyte solutions. Moreover, the activation energy of each sub-relaxation and the ionic conduction of PAA-*g*-PEO-*g*-dodecyl solutions were calculated, and it was found that the free counterions participate in the ionic conduction process, but the condensed counterions do not.

By the systematic investigation on the conformation, the counterion distribution and the ionic conduction in aqueous solution of polyelectrolyte containing hydrophilic/hydrophobic side-chains, the results in this work may provide some theoretical and experimental support for the fundamental research of polyelectrolyte solution and its application.

Acknowledgements

The authors would like to thank Dr Jin-kun Hao (The Institute of Chemistry, The Chinese Academy of Science, China) for supplying the sample used in this experiment. The financial support from the National Natural Scientific Foundation of China (No. 21173025, 21473012) and the Major Research Plan of NSFC (No. 21233003) are gratefully acknowledged.

References

1 M. Itakura, K. Inomata and T. Nose, *Polymer*, 2001, **42**, 9261.
2 H. Morinaga, H. Morikawa, Y. Wang, A. Sudo and T. Endo, *Macromolecules*, 2009, **42**, 2229–2235.
3 L. Gu, Z. Shen, C. Feng, Y. Li, G. Lu and X. Huang, *J. Polym. Sci., Part A: Polym. Chem.*, 2008, **46**, 4056.
4 H. Yamamoto and Y. Morishima, *Macromolecules*, 1999, **32**, 7469–7475.
5 J. Hao, Z. Li, H. Cheng, C. Wu and C. C. Han, *Macromolecules*, 2010, **43**, 9534.
6 D. Schmaljohann, *Adv. Drug Delivery Rev.*, 2006, **58**, 1655–1670.
7 K. E. Uhrich, S. M. Cannizzaro, R. S. Langer and K. M. Shakesheff, *Chem. Rev.*, 1999, **99**, 3181.
8 J. L. Barrat and J. F. Joanny, Theory of polyelectrolyte solutions, *Adv. Chem. Phys.*, 1996, **94**, 1–66.
9 A. V. Dobrynin and M. Rubinstein, *Prog. Polym. Sci.*, 2005, **30**, 1049–1118.
10 O. Trotsenko, Y. Roiter and S. Minko, *Langmuir*, 2012, **28**, 6037–6044.
11 J. Kłos, *J. Chem. Phys.*, 2005, **122**, 134908.
12 C. Keyes-Baig, M. Mathew and J. Duhamel, *J. Am. Chem. Soc.*, 2012, **134**, 16791.
13 V. M. Prabhu, *Curr. Opin. Colloid Interface Sci.*, 2005, **10**, 2–8.
14 A. V. Dobrynin, R. H. Colby and M. Rubinstein, *Macromolecules*, 1995, **28**, 1859.
15 A. G. Cherstvy, *J. Phys. Chem. B*, 2010, **114**, 5241–5249.
16 G. S. Manning, *J. Chem. Phys.*, 1969, **51**, 924.
17 Q. Liao, A. V. Dobrynin and M. Rubinstein, *Macromolecules*, 2003, **36**, 3399–3410.
18 F. Bordi, R. Colby, C. Cametti, L. De Lorenzo and T. Gili, *J. Phys. Chem. B*, 2002, **106**, 6887.
19 K. Ito, A. Yagi, N. Ookubo and R. Hayakawa, *Macromolecules*, 1990, **23**, 857.
20 F. Bordi, C. Cametti and R. Colby, *J. Phys.: Condens. Matter*, 2004, **16**, R1423.
21 Y. Ono and T. Shikata, *J. Am. Chem. Soc.*, 2006, **128**, 10030.
22 G. Masci, S. De Santis and C. Cametti, *J. Phys. Chem. B*, 2011, **115**, 2196–2204.
23 M. Mandel and T. Odijk, *Annu. Rev. Phys. Chem.*, 1984, **35**, 75–108.
24 F. Bordi, C. Cametti, T. Gili and R. Colby, *Langmuir*, 2002, **18**, 6404.
25 C. Cametti and S. Zuzzi, *J. Phys. Chem. B*, 2010, **114**, 7140.
26 C. Y. Liu and K. S. Zhao, *Soft Matter*, 2010, **6**, 2742.
27 T. Vuletić, S. D. Babić, T. Ivek, D. Grgičin, S. Tomić and R. Podgornik, *Phys. Rev. E: Stat., Nonlinear, Soft Matter Phys.*, 2010, **82**, 011922.
28 J. L. Li and K. S. Zhao, *J. Phys. Chem. B*, 2013, **117**, 11843–11852.
29 H. Schwan, Determination of biological impedances, in *Physical Techniques in Biological Research*, ed. W. L. Nastuk, Academic Press, Inc., New York, 1963.
30 M. Stoneman, M. Kosempa, W. Gregory, C. Gregory, J. Marx, W. Mikkelson, J. Tjoe and V. Raicu, *Phys. Med. Biol.*, 2007, **52**, 6589.
31 Q. Liao, A. V. Dobrynin and M. Rubinstein, *Macromolecules*, 2003, **36**, 3386–3398.
32 J. Hao, *Study on the mechanisms of the collapse/association of smart polymer: [D]*, The Institute of Chemistry, Beijing, 2010.
33 E. A. Litmanovich, S. O. Zakharchenko and G. V. Stoichev, *J. Phys. Chem. B*, 2007, **111**, 8567.
34 F. Bordi, C. Cametti, T. Gili, S. Sennato, S. Zuzzi, S. Dou and R. Colby, *Phys. Rev. E: Stat., Nonlinear, Soft Matter Phys.*, 2005, **72**, 031806.
35 L. Longsworth, *J. Phys. Chem.*, 1954, **58**, 770.
36 C. Liu and K. Zhao, *J. Phys. Chem. B*, 2012, **116**, 763.
37 F. Van der Touw and M. Mandel, *Biophys. Chem.*, 1974, **2**, 231.
38 S. Koneshan, R. Lynden-Bell and J. C. Rasaiah, *J. Am. Chem. Soc.*, 1998, **120**, 12041.
39 C. Cametti, S. Marchetti, C. Gambi and G. Onori, *J. Phys. Chem. B*, 2011, **115**, 7144.
40 G. H. Koenderink, H. Zhang, D. G. Aarts, M. P. Lettinga, A. P. Philipse and G. Nägele, *Faraday Discuss.*, 2003, **123**, 335.